18

Luminescent properties of colloidal Ag_2 quantum dots passivated with thioglycolic acid molecules in the presence of oxytetracycline

© T.S. Kondratenko, T.A. Chevychelova, O.V. Ovchinnikov, M.S. Smirnov, I.G. Grevtseva, A.N. Latyshev

Voronezh State University, Voronezh, Russia

e-mail: optichka@yandex.ru

Received November 26, 2025
Revised November 26, 2025
Accepted December 26, 2025

It was found that in the presence of oxytetracycline molecules, the spectral absorption and luminescence contours of colloidal Ag_2S quantum dots, passivated with thioglycolic acid molecules are transformed. During mixing a colloidal solution of Ag_2S/TGA quantum dots with antibiotic molecules, a peak at 2.5 ± 0.2 nm appears in the absorption spectrum, and a luminescence peak shift to shorter wavelengths (from 940 nm to 860 nm) is observed in the luminescence spectrum, accompanied by an increase in its intensity. The observed regularities are caused by a change in the interface state of Ag_2S/TGA quantum dot due to binding with the oxytetracycline molecule through the interaction of the tricarbonyl group with dangling bonds of the quantum dot interface and passivator molecules. It ensures the formation of new radiative recombination centers. The obtained results indicate the possibility of practical application of colloidal solution of Ag_2S/TGA quantum dots as a luminescent receptor for the presence of tetracycline antibiotics in solution.

Keywords: trap-state luminescence, Ag_2S quantum dots, oxytetracycline, interface.

DOI: 10.61011/EOS.2026.01.63226.8801-25

Introduction

The widespread use of antibiotics and their uncontrolled use in some cases poses a serious threat to the environment and human health [1,2]. Therefore, it becomes more urgent to develop new, simple and cheap sensors capable of easy and accurate detection of the trace concentrations of antibiotics in the environment, and especially in food products. Today, sensory problems of this kind are solved by high performance liquid chromatography (HPLC) [3,4], mass spectrometry (MS) [3,5], enzyme-linked immunoassay [3,6]. However, these methods require expensive equipment and special pre-sample preparation. Effective quick analysis is possible using luminescent sensors [7–26]. Recently, the development of luminescent sensors' sensitive elements based on colloidal quantum dots (QD) has been increasingly recognized as a promising approach [7–16]. Due to a developed multifunctional interface, a selective reaction to the antibiotic in a sample is likely to occur, resulting in the activation of non-radiative energy transfer of electronic excitation or photo-transfer of charge carriers (formation or dissociation of a non-luminescent complex). In this case, high concentration sensitivity is achieved by associating an antibiotic molecule (analyte) with a sensitive element (receptor) of a luminescent sensor. Commonly used QD interface passivation molecules for polar media (any biological fluids, water, milk, etc.) have charged end-groups (COO^-, NH^+) that prevent coagulation of QDs in a solution. These interface charges may also prevent the antibiotic from attaching to QDs, making the process of targeting of a sensor element to an analyte somewhat problematic. Higher binding strength of the antibiotic to QD is achieved with the help of metal ions capable of forming coordination bonds with QD interfaces, including the passivator molecules covering them, as well as with antibiotic molecules of a specific group. In particular, the functionalization of interfaces of semiconductor nanocrystals with size-dependent absorption and luminescent properties by ions of transition and rare-earth metals provides new options for the luminescent sensors [17–25]. Colloidal QDs of various compositions are used to recognize antibiotics in water and other hydrophilic media: carbon, silicon, and compounds of group $A^{II}B^{VI}$ (CDs, CdTe, ZnO, etc.), functionalized with ions of transition and rare earth metals [17–26]. At the same time, the detection limit of sensitive elements of QD luminescent sensors in the presence of transition metal ions (Zn^{2+}, Ni^{2+}) and rare earth ions is as high as 5 pM [17,18,22].

It is important to note that incorporation of impurity metal ions into the lattice of [27–29], as well as the doping of interfaces has a significant effect on the structural and luminescent properties of QD[28,30]. For the semiconductor QD Ag_2S, characterized by high nonstoichiometry of composition and dependence of the properties of recombination luminescence on the interface state [31–34], the optical properties of QDs doped with transition metal ions were individually studied as described in the literature (Cu^{2+}, Ni^{2+}, Mg^{2+}, Co^{2+} and etc.). The available data is usually contradictory [35–37]. The structural, optical, and photoluminescent properties of Ag_2S nanocrystals doped with Cu^{2+}ions synthesized by chemical coprecipitation were studied in [35]. As the concentration of Cu^{2+} ions increased, a small long-wavelength shift (20 nm) and a decrease in

the luminescence intensity of Ag_2S nanocrystals located near 450nm were observed. The effect of doping of Ag_2S nanoparticles synthesized by „wet" chemistry with Mg^{2+} and Ni^{2+} ions is studied in [36], and a different luminescence response to the presence of metal ions is illustrated. For Mg^{2+} ions higher luminescence in QD luminescence band is observed along with the shift of the peak to the long-wavelength side, and for Ni^{2+} — quenching and a short-wavelength shift of the QD luminescence peak. The observed changes are explained by the incorporation of metal ions into the lattice, accompanied by a change in the size and energy structure of the nanoparticles Ag_2S. In the study [37] the selective quenching of Ag_2S QDs luminescence with Fe^{3+}ions was found. However, the luminescent-sensory properties of such structures have not been investigated, nor has the mechanism of transition metal ions impact on the recombination luminescence of colloidal Ag_2S quantum dots been substantiated.

The present study partially fills this gap and aims to clarify the mechanism of Ni^{2+} impact on the luminescent and luminescent-sensory properties of silver sulfide QDs passivated with thioglycolic acid molecules (QD Ag_2S/TGA), with an average size of 2.5 ± 0.2 nm (KT Ag_2S/TGA); the possibility of using these structures as an element of the luminescent sensor sensitive to a tetracycline-type antibiotic in water is investigated using oxytetracycline (OTC) as an example.

Materials and methods

Synthesis of colloidal Ag_2S/TGA QDs and method of Ni^{2+} doping

To get Ag_2S/TGA QDs in an aqueous solution, the original synthesis method of [31,38,39] was used, based on mixing two solutions of precursors Ag^+ and S^{2-}. As a first precursor they used a mixture of water solutions $AgNO_3$ ($3 \cdot 10^{-2}$ M) and TGA ($1.5 \cdot 10^{-2}$ M) at pH 10. Water solution of sodium sulfide Na_2S ($2.6 \cdot 10^{-2}$ M) was used as a second precursor. The second solution was drip-injected into the first one with constant stirring and controlling pH of the medium. The resulting mixture was kept for a day at room temperature. To purify the colloid from the reaction products, it was dispersed in acetone in the volumetric ratio 1 : 1, centrifuged, freed from liquid, and the resulting powder was dissolved in distilled water. The resulting colloidal solution had pH 8.

Doping the interfaces of Ag_2S/TGA QDs with Ni^{2+} ions (QD Ag_2S/TGA : Ni^{2+}) was accomplished by adding the nickel ions precursor $NiCl_2$ (10^{-2} M) into a colloidal solution containing QD Ag_2S/TGA ($5 \cdot 10^{-3}$ M, 10 mL), in the volumes providing different percentage ratios in terms of metal: $w(\mathrm{Ni/Ag}) = 1, 2, 5, 8, 10\%$.

Getting model samples of OTC water solutions

Aqueous solutions of OTC were obtained in various concentrations from $0.2 \cdot 10^{-6}$ M to 10^{-3} M. Preparation of mixtures QD Ag_2S/TGA : Ni^{2+} with OTC antibiotic molecules was performed by injecting an aqueous solution of OTC in various concentrations in a volume of 100 μL into a colloidal solution of QD, ensuring the content of OTC in the solution of $9.5 \cdot 10^{-9}$ M to $5 \cdot 10^{-5}$ M.

Research procedures

The structural properties of the obtained samples were studied using transmission electron spectroscopy (TEM) on microscope Libra 120 (CarlZeiss, Germany) with an accelerating voltage of 120 kV and a transmission electron microscope JEM-2100 (Jeol, Japan) with an accelerating voltage of 200 kV in case of high-resolution electron microscopy, as well as energy-dispersive X-ray analysis (EDX) using a spectrometer integrated into transmission electron microscope Libra 120 PLUS (Carl Zeiss, Germany).

The absorption properties were studied using USB2000+ spectrometer (Ocean Optics, USA) with a USB-DT continuous radiation source (Ocean Optics, USA).

Stationary luminescence spectra from 700 to 1400 nm were detected with a spectral complex based on a diffraction monochromator MDR-4 (LOMO, Russia) and a near-infrared photodetector PDF10C/M (ThorlabsInc., USA). Photoluminescence was excited by a GH0782RA2C laser diode (China) with a wavelength of 780 nm and an optical power of 200 mW.

To register the luminescence excitation spectra, the same spectral complex was used, only an incandescent lamp with a power of 400 W and a second monochromator with a 1200 mm grating were used as the excitation source. $^{-1}$, thus, providing an excitation region from 500 to 1300 nm with s step of 1 nm.

To study the dynamics of luminescence decay in the band Ag_2S/TGA QD and structures based on them Ag_2S/TGA : Ni^{2+} PicoSingleTCSPC system for time-correlated counting of photons was used with a InGaAsKIT-IF-25C single-photon detector (MicroPhotonDevices, Italy) and additional photomultiplier module PMC-100-20 with controller (Becker & Hickle) providing the system sensitivity in the region of up to 400–1400 nm. A PICOPOWERLD660 semiconductor pulse laser was used as an excitation source (with a wavelength of 660 nm, a pulse length of 60 ps) (Alphalas, Germany). Time resolution of this setup configuration was 0.2 ns and limited by characteristics of the single-photon detector.

IR absorption spectra were recorded using FTIR-spectrometer Tensor 37 (Bruker Optik GmbH, Germany). For the study of IR absorption spectra, colloidal quantum dots of Ag_2S/TGA and structures based on them Ag_2S/TGA : Ni^{2+} were applied on KCl wafers and dried as quickly as possible, preventing severe degradation of the

substrates. The deposited solutions had equal volumes and deposition temperatures.

Results and discussion

Structural characteristics of samples

As can be seen from TEM the synthesized Ag_2S/TGA QD have average size in the ensemble of 2.5 ± 0.2 nm with the dispersion 15–20% in size (Fig. 1, *a,b*). High-resolution TEM images (HR-TEM) of synthesized samples showed electron diffraction mainly from the crystallographic plane (121) (Fig. 1, *c*), indicating the formation of Ag_2S nanocrystals with interatomic distances of 0.267 nm in the monoclinic lattice (spatial group $P21/c$). In case of doping of Ag_2S QD interfaces with nickel ions Ni^{2+}, no change in the average size and structure of nanocrystals was observed.

The analysis of EDX results for the regions where TEM images were obtained showed the presence of intense peaks from O and C atoms in the spectra of Ag_2S/TGA : Ni^{2+} QD samples (in addition to the emission lines (Fig. 1, *d*) and these peaks were present in the passivators molecules and the amorphous carbon substrate used, peaks from Ni in the spectral ranges 0.849, 7.480 and 8.264keV, which indicates the presence of nickel in the sample.

Spectral regularities of Ag_2S/TGA : Ni^{2+} QD nanostructures

Optical absorption and luminescence spectra were studied for Ag_2S/TGA QD, the interfaces of which were doped with Ni^{2+} ions (Fig. 2, *a*). In the spectra of optical absorption of quantum dots Ag_2S/TGA and Ag_2S/TGA : Ni^{2+} a wide structureless band with its edge in 780–850 nm was observed. The absence of a pronounced exciton structure in the optical absorption spectrum of these samples is probably a consequence of QD dispersion in size (15–20% according to TEM image analysis) and the nonstoichiometry of Ag_2S nanocrystals [31,40]. Luminescence excitation spectra are more sensitive to optical transitions in absorption. In the luminescence excitation spectra of the samples, the peak was observed in the region of 800 nm (1.55 eV) (Fig. 2, *a*). If doped with Ni^{2+} ions Ag_2S/TGA QD interfaces, the maximum in the luminescence excitation spectrum became more pronounced and practically did not experience a spectral shift.

The energy of the main exciton transition in absorption, determined from the luminescence excitation spectrum for the studied QD samples of Ag_2S/TGA ($E_g^{\text{ef}} = 1.55$ eV), exceeded the band gap for massive crystals Ag_2S with a monoclinic crystal structure at 0.46 eV (1.09 eV) [40], due to the quantum-dimensional effect. Estimation of the average QD size using Bruce formula [41]

$$E_g^{\text{ef}} = E_g + \frac{\hbar^2 \pi^2}{2R^2 \mu} - \frac{1.8e^2}{\varepsilon R}, \qquad (1)$$

Luminescent curves parameters

Sample	E_g^{ef}, eV	$\lambda_{\max}$, nm (eV)	Stokes shift, eV	FWHM, eV	τ, ns
Ag_2S/TGA	1.55	1000 (1.24)	0.31	0.35	3.2
Ag_2S/TGA:Ni^{2+} (1%)	1.55	1000 (1.24)	0.31	0.32	3.8
Ag_2S/TGA:Ni^{2+} (2%)	1.55	930 (1.33)	0.22	0.37	4.7
Ag_2S/TGA:Ni^{2+} (5%)	1.55	930 (1.33)	0.22	0.38	5.2

where $\hbar$ — Planck constant, E_g^{ef} — effective band gap values for QD, E_g — massive crystal band gap (1.09 eV [40]),

$$\mu = \frac{m_{\text{e}}^* m_{\text{h}}^*}{m_{\text{e}}^* + m_{\text{h}}^*}$$

— reduced effective mass for the appropriate crystal, $m_{\text{e}} = 0.42m_0$, $m_{\text{h}} = 0.81m_0$ [40], gave a value of 2.5 nm which correlated with TEM data.

The luminescence spectra of Ag_2S/TGA QD varied more significantly when doped with Ni^{2+} ions at their interfaces. A wide luminescence band in the region of 1000 nm (width at FWHM = 0.35 eV) for Ag_2S/TGA QD (Fig. 2, it b) experienced a significant Stokes shift (about 0.4 eV) relative to position of the most probable transition in optical absorption. A significant Stokes shift exceeding the exciton binding energy for Ag_2S QD (about 0.16 eV) and a significant half-width of the luminescence spectrum indicate the recombination nature of the observed luminescence [31]. The main mechanism of the observed luminescence is the recombination of a free hole with a localized electron at the impurity level — luminescence center [31].

When the interfaces of Ag_2S/TGA QD were doped with Ni^{2+} ions from a solution at the lowest concentration of (1%), luminescence quenching with a peak of about 1000 nm by 50% was observed. As the concentration of the solution grew to 2%, a short-wave shift of the maximum luminescence of Ag_2S/TGA QD to 930 nm and an increase in its intensity by 28% were observed. An increase in the concentration of Ni^{2+} ions doping the interfaces in a colloidal solution to 5% gives a higher intensity of the luminescence band (930 nm) to almost a 10% higher value compared to the luminescence of initial sample of Ag_2S/TGA QD in the band 1000 nm. At that, FWHM practically remains the same: FWHM = 0.38 eV. A further increase in the concentration of Ni^{2+} to 8% leads to the complete extinguishing of the band (Fig. 2, *b*). We should stress here, that the luminescence band for Ag_2S/TGA QD in the presence of nickel is apparently not elementary. This is especially noticeable for sample with 5% of added nickel. The luminescence spectrum clearly shows a singularity in the 1100 nm region, which is probably due to the existence of two types of luminescence centers. One of them includes the recombination luminescence centers initially formed in Ag_2S/TGA QD, and the other contains initial recombination luminescence centers modified with

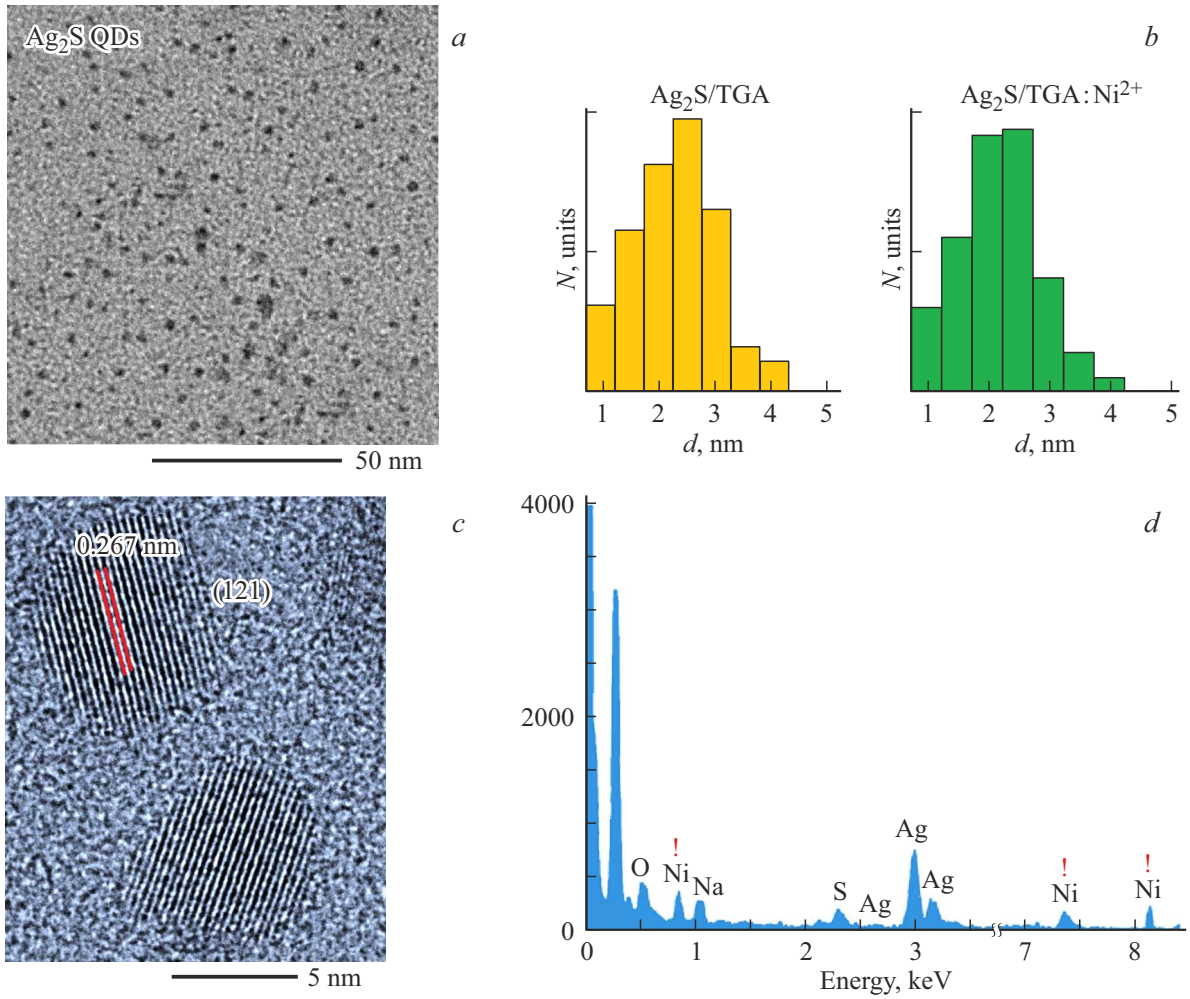

Figure 1. TEM image of Ag_2S/TGA QD ensemble (*a*), distribution hystograms on sizes of Ag_2S/TGA QD and Ag_2S/TGA:Ni^{2+} QD (*b*), high-resolution TEM image (HR−TEM) for Ag_2S/TGA QD ensemble (*c*), results of energy-dispersive X-ray analysis (EDX) of Ag_2S/TGA:Ni^{2+} QD(*d*).

Ni^{2+} ions (Fig. 3, *b*). Thus, the doping of Ag_2S/TGA QD interfaces with Ni^{2+} ions changes the luminescence band FWHM within 0.03 eV, and the Stokes shift declines by 0.09 eV (Fig. 2, *b*, table).

When the Ag_2S/TGA QD interfaces were doped with Ni^{2+} ions, not only the spectral composition of the luminescence, but also the kinetics of luminescence changed. The luminescence decay curves in the bands 930 nm and 1000 nm are shown in Fig. 2, *b* (inset). They turned out to be non-exponential. The average luminescence decay time for Ag_2S/TGA QD and structures of Ag_2S/TGA:Ni^{2+} QD was obtained by approximating the experimental luminescence decay curves by the expression

$$\langle \tau \rangle = \frac{\sum_{i=1}^{2} a_i \tau_i}{\sum_{i=1}^{2} a_i}, \qquad (2)$$

where a_i — amplitude and τ_i — and time constant of i component in the luminescence decay curve. The best consistency on the values of a_i and τ_i were obtained by approximating the luminescence decay curves by the sum of the three exponents:

$$I(t) = \sum_{i=1}^{2} a_i \exp[t/\tau_i]. \qquad (3)$$

The obtained values of the average luminescence decay time are also shown in the table below. As the concentration of the interface doping ions increased, the luminescence decay time increased from 3.8 to 5.2 ns. The same order of average decay time indicates its uniform recombination nature due to transitions at the levels of Ag_2S/TGA QD interface defects [31,33,38,39]. In its turn, higher average lifetime is rather an evidence of co-passivation of Ag_2S/TGAQD interfaces and a decreased concentration of luminescence quenching channels [33,42].

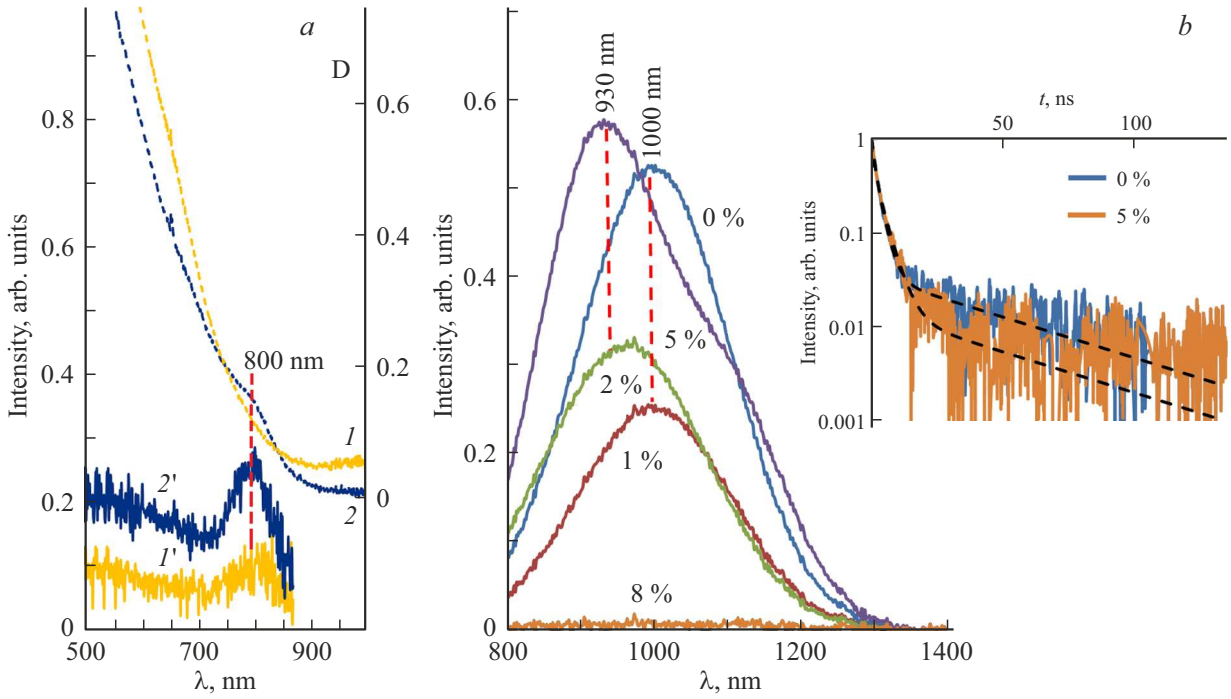

Figure 2. Spectra of absorption (dashed line), luminescence excitation (solid line) of the quantum dots Ag_2S/TGA (*1*, *1′*) and Ag_2S/TGA : Ni^{2+} (*2*, *2′*) (a) and luminescence kinetics of Ag_2S/TGA QD at various concentrations Ni^{2+} (*b*).

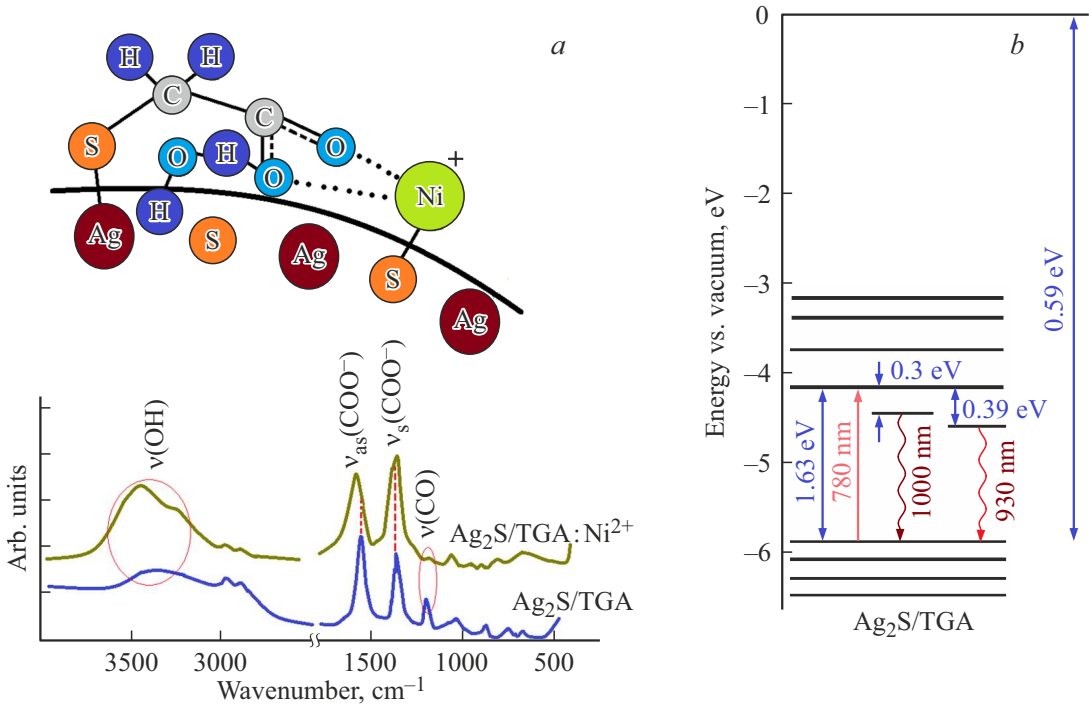

Figure 3. IR absorption spectra of the studied samples (*a*) and diagram of the photo-processes in Ag_2S QD (*b*).

Since the nickel precursor was introduced into the solution of Ag_2S/TGA QD that had already completed their formation, and the average size of the nanocrystals did not noticeably change, it can be assumed that Ni^{2+} ions are not embedded in the volume, but are adsorbed on interfaces. The interaction can be carried out both with broken QD bonds (S^{2-}) and with passivator molecules (functional group COO^- in TGA molecule).

Fig. 3, *a* illustrates the IR absorption spectra of Ag_2S/TGA QD before and after doping of interfaces with Ni^{2+} ions. To

decipher the observed patterns in the IR absorption spectra, we will use the data of paper [39]. For Ag_2S/TGA QD, a detailed analysis of IR absorption spectra, as in[39], showed that TGA molecules at the interfaces of Ag_2S nanocrystals are adsorbed as a configuration with free and reactive carboxylate- anion (COO^-) (Fig. 3, *a*, curve *1*), which is characterized by asymmetric ($1565\,cm^{-1}$) and symmetric ($1385\,cm^{-1}$) stretching of COO^- group, as well as $-O-$ stretching ($1489\,cm^{-1}$). When Ag_2S/TGA QD interfaces are doped with Ni^{2+} ions, the most noticeable changes are observed in the region of these oscillations. A shift of peaks corresponding to the asymmetric ($1565\,cm^{-1}$) and symmetric ($1385\,cm^{-1}$) stretching of COO^- group, a lower intensity of the band of C−O-stretching ($1489\,cm^{-1}$). In addition, there are changes in the stretching of OH groups: a shift in a singularity corresponding to OH stretching included in hydrogen bonds ($3200\,cm^{-1}$). The observed changes indicate the involvement of hydrogen bonds in the interaction of the passivating ligand TGA with QD interfaces, including in conditions of doping with Ni^{2+} ions.

Thus, IR absorption spectroscopy data confirm a change in the structure of the Ag_2S/TGA QD interfaces when they are doped with Ni^{2+} ions (Fig. 3, *a*). In addition to binding to TGA ligand molecules, Ni^{2+} ions are able to interact with dangling bonds of the interface of Ag_2S nanocrystals. Such diagram of metal-QD interface interaction is given in Fig. 3, *a* (inset).

The depth of the level of Ni^{2+} ion adsorbed over the anion of Ag_2S QD interface was estimated using a semi-empirical method for determining the energy state of an adsorbed atom or ion on the surface of an ion-covalent crystal, proposed in [34,97,98]. This model is based on the assumption that the electron that binds the atom to the lattice does not penetrate deep into the crystal, but is localized near the emerging bond. The expression for the optical depth of the level associated with Ni^{2+} adsorbed over the surface anion is given as

$$E_{\text{anion}} = \frac{E_g^{\text{exp}}}{2}\,\frac{\Gamma - \frac{1}{4Cz}\,\frac{n^2-1}{n^2+1}}{1-\mu}, \qquad (4)$$

where

$$\mu = \frac{I-A}{2Cze^2}\,n_0$$

$E_g^{\text{exp}} = 1.55\,\text{eV}$ — experimental band gap value, $n = 2.2$ [43–46] — high-frequency refractive index value, $\varepsilon = 7.77$ [47] — low frequency value of dielectric permittivity, $\Gamma = 0.57$ — geometric factor depending on the crystal surface indices calculated for the surface (031), $r_0 = 2.5 \cdot 10^{-8}\,\text{cm}$ [40] — distance between the nearest lattice ions, $C = 3.03$ — Madelung constant found by Ewald method [48], $z = 0.63$ — effective ion charge of the crystal, taking into account the partial covalence of the crystal, estimated under Gorsky−Gorodetsky model [49], $e = 4.8 \cdot 10^{-10}\,\text{erg}$ — electron charge, $I = 7.58\,\text{eV}$ [50] — ionization potential of the silver atom of the lattice, $A = 2.077\,\text{eV}$ [50] — affinity to the electron of the sulfur atom, $d = 2.5\,\text{eV}$ [50] — binding energy of the atom adsorbed to the crystal.

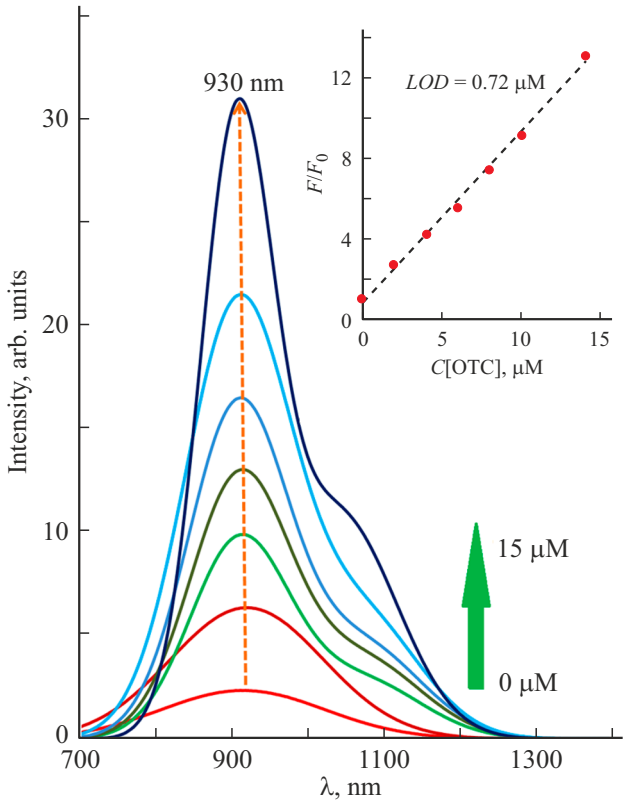

Figure 4. Luminescence spectra of Ag_2S/TGA : Ni^{2+} QD mixtures with OTC registered at various concentrations of the antibiotic in the aqueous solution. Inset — dependence between the fluorescent response (F_0/F) and concentration of OTC (C [OTC]).

The depth of the localized state turned out to be $E_{\text{cation}} = 0.64\,\text{eV}$. Comparing the depth of this trap with the depth of the luminescence center, calculated from the minimum value of the conduction state, demonstrates their proximity and indicates the difficulty of unambiguously establishing the role of Ni^{2+} ions in the formation of luminescent properties of Ag_2S/TGA QD with their interfaces doped with Ni^{2+}.

QD of Ag_2S/TGA : Ni^{2+} for the luminescence detection of OTC

Luminescent sensory properties were studied for Ag_2S/TGA QD samples, the interfaces of which were doped with Ni^{2+} ions. It was assumed that during luminescent detection of OTC antibiotic molecules in water, Ni^{2+} ions should act as a targeting agent forming coordination complexes with them [51].

Figure 4 shows the luminescence spectra of mixtures of Ag_2S/TGA : Ni^{2+} QD in the presence of OTC in an aqueous solution with their concentration varying within $0-15\,\mu M$. It can be seen that the luminescence intensity in the band near 930nm gradually rises with an increase

in concentration of OTC added to the colloidal solution of QD $Ag_2S/TGA:Ni^{2+}$. The extinguishing efficiency was estimated from F_0/F versus quencher concentration C [OTC] in accordance with the principles of Stern–Volmer equation [52]:

$$\frac{F_0}{F} = 1 + K_{SV}\,C[\mathrm{OTC}], \tag{5}$$

where F_0 — intensity of glow in 930 nm band in the absence of OTC, F — intensity of glow of QD + OTC in mixture 930 nm, K_{SV} — Stern–Volmer constant, C [OTC] — concentration of quencher (antibiotic).

F_0/F versus concentration of antibiotic (C [OTC]) in the mixture of QD $Ag_2S/TGA:Ni^{2+}$ with OTC is itself a linear function within concentrations interval $0-15\,\mu$M, which is expressed as $F_0/F = 1 + 0.848C$ [OTC] ($R^2 = 0.992$) (Fig. 4). Further, the dependence of F_0/F on the concentration in $0-15\,\mu$M was used as the calibration curve of the luminescent sensor. For this interval the limit of detection OTC (LOD) and limit of quantification (LOQ) (Limit of Detection (LOD) and Quantification (LOQ)), were defined using the standard ratios

$$\mathrm{LOD} = 3.3\,\frac{\sigma}{K}, \tag{6}$$

$$\mathrm{LOQ} = 10\,\frac{\sigma}{K}, \tag{7}$$

where σ — standard deviation, K — slope of the graduation curve. The detection limit calculated from the calibration curve (Fig. 4, inset) was $0.72\,\mu$M, the limit of quantification $\mathrm{LOQ} = 1.36\ \mu$M.

The results obtained indicate the option of practical application of a colloidal solution of $Ag_2S/TGA:Ni^{2+}$ quantum dots as an element of a luminescent sensor sensitive to OTC presence in the solution, and aimed at enhancing the luminescent signal in a 930 nm band when the concentration of antibiotic molecules rises in the linear concentration range $0-15\,\mu$M, with a detection limit of $\mathrm{LOD} = 0.72\ \mu$M.

Conclusion

This study describes the effect of nickel ions on the luminescent properties of colloidal Ag_2S QD passivated with thioglycolic acid molecules with an average size of 2.5 ± 0.2 nm (Ag_2S/TGA QD) and the sensory properties of QD structures $Ag_2S/TGA:Ni^{2+}$ with respect to oxytetracycline in water. As a result of doping, the recombination luminescence band of Ag_2S/TGA QD (1000 nm) is extinguished and the 930 nm band is ignited, which is also extinguished at concentrations of w(Ni/Ag) by more than 5%. The observed patterns in the spectra of recombination luminescence of Ag_2S/TGA QD are explained by a complex mechanism of Ni^{2+} ions effect on the structure of QD interface during their adsorption, including formation of non-luminescent complexes, co-passivation of the nanocrystal interface, and modification of the recombination glow center. The observed empirical patterns are in good agreement with theoretical estimates for the energy states of QD levels within semi-empirical calculation method of the adsorbed atom (ion) model.

It was shown by experiment that QDs of $Ag_2S/TGA:Ni^{2+}$ are a promising luminescent sensor element sensitive to the presence of oxytetracycline in water with a limit of detection $\mathrm{LOD} = 0.72\,\mu$M within the linear range of $0-15\,\mu$M.

Funding

This work was supported by the Russian Science Foundation (project № 24-29-00668).

Conflict of interest

The authors declare that they have no conflict of interest.

References

[1] N.S. Antropova, O.V. Ushakova, O.N. Savostikova, E.I. Filimonova. Zdorovie naseleniya i sreda obitaniya , **32** (3), 33 (2024) (in Russian). DOI: 10.35627/2219-5238/2024-32-3-33-43

[2] S. Sachi, J. Ferdous, M.H. Sikder, S.M.A.K. Hussani. JAVAR, **6** (3), 315 (2019). DOI: 10.5455/javar.2019.f350

[3] O.I. Lavrukhina, V.G. Amelin, L.K. Kish, A.V. Tretyakov, T.D. Penkov. Zhurnal analiticheskoy khimii, **77** (11), 969 (2022) (in Russian). DOI: 10.31857/S004445022211007X

[4] P. Moudgil, J.S. Bedi, R.S. Aulakh, J.P.S. Gill, A. Kumar. Food Anal. Methods, **12**, 338 (2018). DOI: 10.1007/s12161-018-1365-0

[5] S.H. López, J. Dias, A. de Kok. Food Control, **115**, 1873 (2020). DOI: 10.1016/j.foodcont.2020.107289

[6] N.E.A. El Hassani, A. Baraket, S. Boudjaoui, E.T.T. Neto, J. Bausells, N. El Bari, B. Bouchikhi, A. Elaissari, A. Errachid, N. Zine. Bioelectron., **130**, 330 (2019) DOI: 10.1016/j.bios.2018.09.052

[7] X.-Y. Zhang, Y.-S. Yang, W. Wang, Q.-C. Jiao, H.-L. Zhu. Coordination Chem. Rev., **417**, 213367 (2020). DOI: 10.1016/j.ccr.2020.213367

[8] A. Loskutova, A. Seitkali, D. Aliyev, R. Bukasov. Int. J. Mol. Sci., **26**, 6674 (2025). DOI: 10.3390/ijms26146674

[9] F. Liu, C. Zhu, Y. Wang, Y. Zhang. J. Fluorescence, **34** (3), 1183 (2023). DOI: 10.1007/s10895-023-03360-7.

[10] Z. Zhang, H. Zhang, D. Tian, A. Phan, M. Seididamyeh, M. Alanazi, Z. Ping Xu, Y. Sultanbawa, R. Zhang. Coordination Chem. Rev., **498**, 215455 (2024). DOI: 10.1016/j.ccr.2023.215455

[11] M.M. Sabzehmeidani, M. Kazemzad. Sci. Total Environment, **810**, 151997 (2022). DOI: 10.1016/j.scitotenv.2021.151997

[12] R. Ding, Y. Chen, Q. Wang, Z. Wu, X. Zhang, B. Li, L. Lin. J. Pharmaceutical Analysis, **12** (3), 355 (2022). DOI: 10.1016/j.jpha.2021.08.002

[13] H. Elmizadeh, M. Soleimani, F. Faridbod, G. R. Bardajee. J. Photochem. Photobiol. A: Chemistry, **367**, 188 (2018). DOI: 10.1016/j.jphotochem.2018.08.021

[14] W. Li, K. Luo, M. Lv, Y. Wen. J. Nanoparticle Research, **26** (4), 70 (2024). DOI: 10.1007/s11051-024-05977-6

[15] F. Liu, C. Zhu, Y. Wang, Y. Zhang. J. Fluorescence, **34** (3), 1183 (2023). DOI: 10.1007/s10895-023-03360-7
[16] Y. Fu, L. Huang, S. Zhao, X. Xing, M. Lan, X. Song. Spectrochim. Acta Part A: Molecular and Biomolecular Spectroscopy, **246**, 1386 (2021). DOI: 10.1016/j.saa.2020.118947
[17] M. Khawla, H. Zouhour, C. Yves, H. Souhaira, M. Rym. Opt. Materials, **125**, 112103 (2022). DOI: 10.1016/j.optmat.2022.112103
[18] C. Wu, T. Zhou, Z. Gao, M. Li, Q. Zhou, W. Zhao. Microchem. J., **194**, 109283 (2023). DOI: 10.1016/j.microc.2023.109283
[19] L. Zhu, Q. Wu, X. Mei, Y. Li, J. Yang. Advanced Composites and Hybrid Materials, **6** (221), 6 (2023). DOI: 10.1007/s42114-023-00805-2
[20] J. Xu, S. Guo, L. Jia, T. Zhu, X. Chen, T. Zhao. Chem. Engineering J., **416**, 127741 (2021). DOI: 10.1016/j.cej.2020.127741
[21] Q. Wang, X. Li, K. Yang, S. Zhao, S. Zhu, B. Wang, J. Yi, Y. Zhang, X. Song, M. Lan. Engineering Chemistry Research, **61** (17), 5825 (2022). DOI: 10.1021/acs.iecr.2c00307
[22] S. Tan, Q. Wang, Q. Tan, S. Zhao, L. Huang, B. Wang, X. Song, M. Lan. Chemosensors, **11** (1), 62 (2023). DOI: 10.3390/chemosensors11010062
[23] X. Li, H. Ma, M. Deng, A. Iqbal, X. Liu, B. Li, W. Liu, J. Li, W. Qin. J. Materials Chemistry C, **5** (8), 2149 (2017). DOI: 10.1039/c7tc00305f
[24] B.I. Salman, A.I. Hassan, A. Al-Harrasi, A.E. Ibrahim, R.E. Saraya. Anal. Chimica Acta, **1327**, 343175 (2024). DOI: 10.1016/j.aca.2024.343175
[25] J. Qi, P. Zhang, T. Zhang, R. Zhang, Q. Zhang, J. Wang, M. Zong, Y. Gong, X. Liu, X. Wu, B. Li. Helion, **10** (11), 31 (2024). DOI: 10.1016/j.heliyon.2024.e32133
[26] Z. Wang, L. Duan, D. Zhu, W. Chen. J. Zhejiang Univ-Sci A, **15** (8), 653 (2014). DOI: 10.1631/jzus.A1400108
[27] A.S. Dotsenko, S.G. Dorofeev, K.O. Znamenkov, D.V. Grigoriev. Mendeleev Commun., **22**, 292 (2012). DOI: 10.1016/j.mencom.2012.11.003
[28] T.D. Bui, Q.L. Nguyen, V.C. Nguyen, T.T. Nguyen, H.P. Dang. Bull. Chem. Reaction Engineering & Catalysis, **20** (2), 359 (2025). DOI: 10.9767/bcrec.20372
[29] M.C. Cao, L.M. Dong, S. Wang, X.X. Jin, X.Y. Zhang. Chalcogenide Lett., **15** (7), 371 (2018). DOI: 10.9767/bcrec.20372
[30] T. Pandey, A. Singh, R.S. Kaundalc, V. Pandey. New J. Chem., **48**, 1009 (2024). DOI: 10.1039/D3NJ05285K
[31] M.S. Smirnov, O.V. Ovchinnikov. J. Lumin., **227**, 117526 (2020). DOI: 10.1016/j.jlumin.2020.117526
[32] W.J. Mir, A. Swarnkar, R. Sharma, A. Katti, K.V. Adarsh, A. Nag. J. Phys. Chem. Lett., **6** (19), 3915 (2015). DOI: 10.1021/acs.jpclett.5b01692
[33] O.V. Ovchinnikov, M.S. Smirnov, S.V. Aslanov. Opt. and spectr., **128** (12), 1926 (2020). DOI: 10.21883/OS.2020.12.50331.206-20
[34] S. V. Aslanov, I. G. Grevtseva, T. S. Kondratenko, A.m. H. Hussein, O. V. Ovchinnikov, M. S. Smirnov, A. N. Latyshev. Opt. and spektr., **133** (1), 82 (2025). DOI: 10.61011/OS.2025.01.59883.7279-24
[35] A. Fakhri, M. Pourmand, R. Khakpour, S. Behrouz. J. Photochem. Photobiol. B, **149**, 78 (2015). DOI: 10.1016/j.jphotobiol.2015.05.013
[36] E.S. Aazam. J. Industrial and Engineering Chemistry, **20**, 4033 (2014). DOI: 10.1016/j.jiec.2013.12.106
[37] L. Liu, L. Ga, J. Ai. Sensing and Bio-Sensing Research, **43**, 25 (2024). DOI: 10.1016/j.sbsr.2024.100624
[38] O.V. Ovchinnikov, I.G. Grevtseva, M.S. Smirnov, T.S. Kondratenko, A.S. Perepelitsa, S.V. Aslanov, V.U. Khokhlov, E.P. Tatyanina, A.S. Matsukovich. Optical and Quantum Electronics, **52** (4), 198 (2020). DOI: 10.1007/s11082-020-02314-8
[39] T.S. Kondratenko, O.V. Ovchinnikov, I.G. Grevtseva, M.S. Smirnov, O. Erina, V. Khokhlov, B. Darinsky, E.P. Tatianina. Materials, **13** (4), 909 (2020). DOI: 10.3390/ma13040909
[40] S.I. Sadovnikov, A.I. Gusev, A.A. Rempel. Phys. Chem. Chem. Phys., **17** (19), 12466 (2015). DOI: 10.1039/c5cp00650c
[41] L.E. Brus. J. Chem. Phys., **80** (9), 4403 (1984). DOI: 10.1063/1.447218
[42] T.S. Kondratenko. Opt. and spectr., **133** (1), 65 (2025). DOI: 10.61011/OS.2025.01.59881.7262-24
[43] M.I.Molotsky, A.N.Latyshev, K.V.Chibisov. Dokl. AN SSSR, **190** (2), 383 (1970) (in Russian).
[44] M.I. Molotsky, A.N. Latyshev. Izv. AN SSSR. Ser. Fiz., **35** (2), 359 (1971) (in Russian).
[45] M.I. Molotskiy, A.N. Latyshev, K.V. Chibisov. J. Phot. Sci., **20** (5), 201 (1972).
[46] A. Haghighatzadeh, M. Kiani, B. Mazinani, J. Dutta. J. Materials Science: Materials in Electronics, **31**, 1283 (2020). DOI: 10.1007/s10854-019-02640-y
[47] C. Lu, S. Du, Y. Zhao, Q. Wang, K. Ren, C. Li, W. Dou. RSC Adv., **11**, 28211 (2021). DOI: 10.1039/d1ra04823f
[48] W.K. Winnett, C.P. Nash. Computers & Chemistry, **10** (3), 229 (1986). DOI: 10.1016/0097-8485(86)80016-X
[49] V.P. Gorskii, M.G. Gorodetskii. JETP, **48** (6), 1723 (1965).
[50] S.S. Batsanov. *Strukturnaya khimiya Fakti i zavisimosti* (Dialog-MGU, M., 2000) (in Russian).
[51] Zy. Wang, L. Duan, Dq. Zhu et al. J. Zhejiang Univ. Sci. A, **15**, 653 (2014). DOI: 10.1631/jzus.A1400108
[52] J.R. Lakowicz. *Principles of Fluorescence Spectroscopy* (Springer, 2006).

Translated by T.Zorina